Overexpression of PDGF-BB decreases colorectal and pancreatic cancer growth by increasing tumor pericyte content

Marya F. McCarty,[1] Ray J. Somcio,[2] Oliver Stoeltzing,[2] Jane Wey,[1] Fan Fan,[2] Wenbiao Liu,[2] Corazon Bucana,[2] and Lee M. Ellis[1,2]

[1]Department of Surgical Oncology and [2]Department of Cancer Biology, The University of Texas MD Anderson Cancer Center, Houston, Texas, USA.

We hypothesized that overexpression of PDGF-BB in colorectal cancer (CRC) and pancreatic cancer cells would result in increased pericyte coverage of ECs in vivo, rendering the tumor vasculature more resistant to antiangiogenic therapy. We stably transfected the cDNA for the PDGF-B into HT-29 human CRC and FG human pancreatic cancer cells. Surprisingly, when HT-29 or FG parental and transfected cells were injected into mice (subcutaneously and orthotopically), we observed marked inhibition of tumor growth in the PDGF-BB–overexpressing clones. In the PDGF-BB–overexpressing tumors, we observed an increase in pericyte coverage of ECs. Treatment of PDGF-BB–overexpressing tumors with imatinib mesylate (PDGFR inhibitor) resulted in increased growth and decreased total pericyte content compared with those in untreated PDGF-BB–overexpressing tumors. In vitro studies demonstrated the ability of VSMCs to inhibit EC proliferation by approximately 50%. These data show that increasing the pericyte content of the tumor microenvironment inhibits the growth of angiogenesis-dependent tumors. Single-agent therapy targeting PDGF receptor must be used with caution in tumors when PDGFR is not the target on the tumor cell itself.

Introduction

Angiogenesis is essential for tumor growth. Angiogenesis is a complex process involving not only EC activation but also crosstalk among multiple cell types (1, 2). ECs are the central cells in angiogenesis, yet recent data suggest that pericytes, periendothelial smooth muscle cells that modulate EC function, are also critical for the development of a mature vascular network (3).

Pericytes serve several important functions. Pericytes regulate vascular function, including vessel diameter (and thus blood flow) and vascular permeability (reviewed in refs. 4, 5). Pericytes also provide mechanical support and stability to the vessel wall and maintain EC survival through direct cell-cell contact and paracrine circuits (6, 7). Another key function of pericytes is to regulate (inhibit) EC growth in order to establish a stable and mature vascular network (8). Abnormalities in pericyte coverage of ECs have been implicated in various diseases. For example, diabetic retinopathy is characterized by detachment of pericytes from the ECs, leading to the development of microaneurysms and subsequent blindness (9).

The role of pericytes within the tumor vasculature is currently an area of intense study. The degree of pericyte coverage of ECs in human tumors is controversial. Benjamin et al. demonstrated that 38% of the vessels within human prostate cancer tumors were associated with pericytes compared with almost 75% in normal tissue (10). Similarly, in glioblastoma multiforme, only 19% of the tumor vessels had associated pericytes (10). Eberhard et al. found that the percentage of ECs associated with pericytes varied according to tumor type; there was 65% pericyte coverage in colon cancer and only 13% in glioblastoma (11). Conversely, Morikawa et al. found that pericytes are present on more than 97% of the vessels within tumors, possibly because of differences in the number of markers used and the thickness of tissue sections (12). Importantly, within many tumor types, pericytes show distinct abnormalities, such as decreased numbers associated with ECs and variable adherence to ECs.

Since pericytes play a role in mediating EC survival (13), they have recently emerged as an important therapeutic target for antiangiogenic therapy (14). Studies of antiangiogenic agents targeting EC survival have demonstrated that these agents result in increased apoptosis in ECs that are *not* associated with pericytes, leading to a relative increase in the proportion of vessels with pericyte coverage (10, 15). These data have led to the hypothesis that pericytes mediate resistance to antiangiogenic therapy. If this hypothesis is correct, targeting both ECs and pericytes would increase the efficacy of antiangiogenic therapy, and in fact, this hypothesis is supported by preclinical studies (14, 16).

The exact molecular mechanism mediating pericyte coverage and its biologic relevance in tumors are currently being investigated. In normal tissue, multiple mediators of pericyte proliferation, migration, and function have been described (reviewed in ref. 17). One important family of growth factors implicated in enhanced proliferation and migration of pericytes is the PDGF family (reviewed in ref. 18). There are 4 known PDGF polypeptides — PDGF-A, PDGF-B, PDGF-C, and PDGF-D — that can form disulfide-linked homodimers or heterodimers. These dimers are expressed by a multitude of different cell types, including activated platelets, macrophages, ECs, osteoclasts, and tumor cells. PDGFs interact with 2 tyrosine kinase receptors, PDGFRα and PDGFRβ. PDGFRβ, the receptor that is highly expressed on pericytes and VSMCs, is the primary receptor for the PDGF-BB homodimer. The interaction between PDGF-BB and PDGFRβ induces receptor activation, downstream signaling, VSMC and pericyte proliferation, and enhanced migration in vitro. Importantly, PDGF-B– and PDGFRβ-knockout mice show a similar phenotype characterized by embryonic-lethal defects such as a lack of pericytes or VSMCs

Nonstandard abbreviations used: CRC, colorectal cancer; MTT, 3-[4,5-dimethylthiazol-2-yl]-2,5-diphenyl tetrazolium bromide.

Conflict of interest: The authors have declared that no conflict of interest exists.

Citation for this article: *J. Clin. Invest.* **117**:2114–2122 (2007). doi:10.1172/JCI31334.

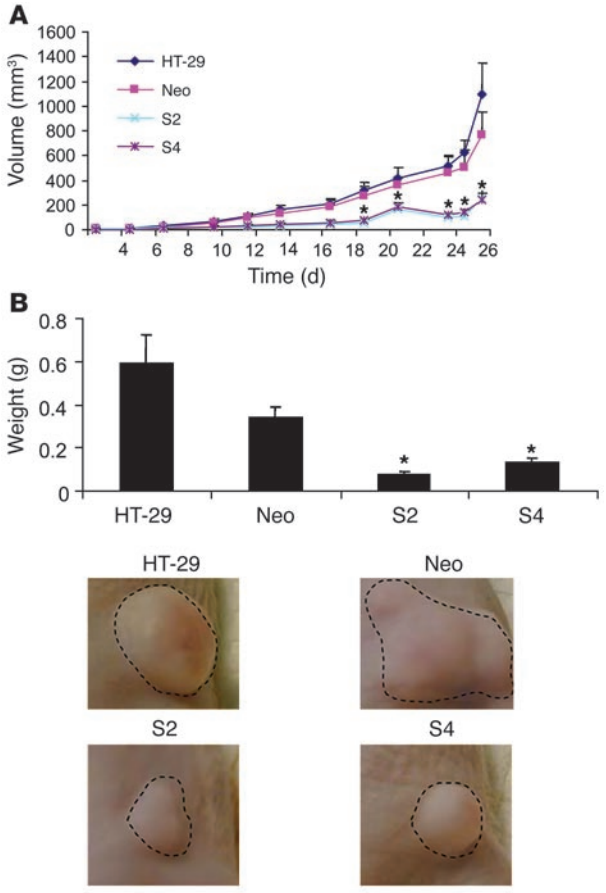

Figure 1
Effect of PDGF-BB overexpression on growth of subcutaneous tumors. Human colon cancer cell lines HT-29 (parental), HT-29 Neo pool, HT-29 S2 (PDGF-BB–overexpressing), and HT-29 S4 (PDGF-BB–overexpressing) (1×10^6) were injected subcutaneously into nude mice. (**A**) Tumor growth was measured 3 times weekly (Monday, Wednesday, and Friday) until tumors became necrotic or larger than 1 cm^3. (**B**) Photomicrographs of representative tumors from each group. HT-29 S2 and HT-29 S4 cells demonstrated decreased tumor growth and a significant reduction in end-stage tumor mass in vivo. *$P < 0.05$. Original magnification, ×1.

leading to widespread hemorrhages and microaneurysms (19, 20). These data suggest the importance of PDGF-BB and PDGF-Rβ in mediating pericyte coverage in normal tissues during development. However, the effect of PDGF-BB on the vasculature, and specifically pericytes, in tumors is not as well understood.

Our initial hypothesis was that pericytes serve as barriers to antiangiogenic therapy that targets ECs. To test this hypothesis, we transfected HT-29 human colorectal cancer (CRC) and FG pancreatic cancer cells with a plasmid encoding the full-length gene for PDGF-B in an effort to increase pericyte coverage of ECs in tumors. However, in the course of this study, we observed some unexpected findings. Surprisingly, PDGF-BB overexpression significantly inhibited in vivo tumor growth both ectopically and orthotopically. Further analysis revealed that PDGF-BB tumors contained an increased proportion of cells that expressed pericyte markers. Confocal microscopy confirmed a high degree of pericyte coverage of ECs in PDGF-BB–overexpressing tumors. Our results suggest that pericytes, through regulation of EC proliferation, may inhibit the angiogenic process in vivo and thus inhibit tumor growth.

Results

Expression of PDGF ligands in control and transfected human cancer cells. Conditioned medium collected from human cancer cell lines (HT-29, KM12L4, KM12SM, GEO, RKO, and FG) after 72 hours of culture was evaluated for PDGF-AA, PDGF-AB, and PDGF-BB ligand expression levels by ELISA. There was no detectable PDGF-AA, PDGF-AB, or PDGF-BB in the conditioned medium from any of the cell lines listed above.

To study the effects of forced expression of PDGF-BB in cancer cells, HT-29 and FG cells were transfected with a plasmid encoding the full-length *PDGFB* gene. Sense clones with various increased levels of PDGF-BB were chosen for further study. More than 25 clones were isolated and evaluated for PDGF-BB expression by ELISA. Two clones of intermediate- and high-expression levels were chosen for each cell line (colon cancer: HT-29 S2 and S4; and pancreatic cancer: FG S1 and S11). HT-29 S2 produced 11 pg of PDGF-BB per 1×10^6 cells per 24 hours, while HT-29 S4 produced 66 pg of PDGF-BB per 1×10^6 cells per 24 hours. HT-29 cells transfected with vector alone (Neo pool cells), similar to HT-29 parental cells, did not produce detectable levels of PDGF-BB. FG S1 produced 2,899 pg of PDGF-BB per 1×10^6 cells per 24 hours, while FG S11 produced 676 pg of PDGF-BB per 1×10^6 cells per 24 hours. FG Neo pool cells, like the FG parental cells, did not produce detectable levels of PDGF-BB. Since PDGF-B transfection can hypothetically lead to an increase in PDGF-AB, an ELISA was performed for PDGF-AB protein levels. The results demonstrated that none of the cell lines (either parental or transfected clones) produced detectable levels of PDGF-AB or PDGF-AA.

To determine whether PDGF-BB can induce autocrine effects in HT-29 cells, the expression of PDGFRα and PDGFRβ was determined by reverse transcription–polymerase chain reaction and Western blotting. HT-29 cells did not express detectable levels of PDGFRα mRNA but did express very low levels of PDGFRβ mRNA and protein (data not shown). This finding is consistent with observations of Kitadai et al. (21), who found that tumor cell PDGFRβ is rarely expressed in human specimens and, when present, is expressed at exceedingly low levels.

Cell proliferation assays were performed to determine whether overexpression of PDGF-BB or addition of exogenous PDGF-BB stimulated HT-29 cell proliferation. There was no significant difference between the doubling times of the HT-29 S2 and HT-29 S4 clones (32 hours and 36 hours, respectively) and HT-29 parental and HT-29 Neo pool cells (27 hours and 31 hours, respectively). There was also no significant difference between the doubling times of the FG S1 clone (40 hours) and the FG parental and FG Neo pool cells (32 and 34 hours, respectively). The addition of exogenous PDGF-BB also did not cause enhanced proliferation (data not shown). FACS analysis confirmed that there was no difference in cell cycle parameters among HT-29 parental, HT-29 Neo pool, and the PDGF-BB–overexpressing HT-29 clones (data not shown).

Effect of PDGF-BB overexpression on HT-29 and FG tumor growth in vivo. To determine the effects of PDGF-BB overexpression on HT-29 cells, we injected cell suspensions into the subcutaneous tissues of nude mice. On day 27, several mice in the control group (parental and Neo pool) became lethargic; the experiment was terminated and all mice were sacrificed. The mean volume

Table 1
Effect of PDGF-BB overexpression on microvessel density, tumor cell proliferation and apoptosis, EC proliferation, and pericyte coverage

	HT–29 P	HT–29 Neo pool	HT–29 S2	HT–29 S4
Microvessel density, no. of vessels/HPF	13.3 ± 2.9	17.4 ± 3.2	7.1 ± 1.7[A]	11.2 ± 1.9[B]
Tumor cell proliferation, no. of cells/HPF	42.4 ± 10.6	54.1 ± 6.1	17.9 ± 5.5[A]	25.0 ± 2.3[B]
Tumor cell apoptosis, no. of cells/HPF	1.6 ± 0.7	3.2 ± 2.0	6.4 ± 1.9	3.0 ± 1.1
EC proliferation, % $CD31^+BrdU^+$ cells/HPF	3.8 ± 0.7	5.3 ± 0.8	2.7 ± 0.7	3.0 ± 0.4
% ECs cells covered by pericytes[C]	31.6 ± 1.7	36.7 ± 4.8	45.8 ± 4.1[D]	48.8 ± 4.6[D]
% Area occupied by pericytes/HPF[E]	6.0 ± 0.8	6.0 ± 0.8	10.8 ± 0.9[A]	9.4 ± 1.6[B]

HT–29 P, HT–29 parental; HPF, high-power field. [A]$P < 0.005$ by Student's t test versus HT-29 Neo pool. [B]$P < 0.04$ by Student's t test versus HT-29 Neo pool. [C]Determined using pericyte marker α-SMA. [D]$P < 0.02$ by Student's t test versus HT-29 P. [E]Determined using pericyte marker NG2.

of the PDGF-BB–overexpressing tumors was less than one-third the mean volume of the HT-29 and HT Neo pool (control vector only) tumors ($P < 0.03$) (Figure 1A). A 5-fold reduction in tumor mass was also observed in the PDGF-BB–overexpressing tumors ($P < 0.03$) (Figure 1B). Animal studies were repeated 2 additional times, and similar results were obtained in each experiment.

To determine whether the tumor growth inhibition observed in HT-29 CRC could be replicated in FG pancreatic cancer, cell suspensions from FG Neo pool and PDGF-B transfected cells (FG S1) were injected subcutaneously into nude mice. On day 49, the experiment was terminated due to large tumor burden in the control group. The mean volume of the FG S1 PDGF-BB–overexpressing tumors was significantly lower than the volume in the control group (FG Neo pool, 954 ± 187 mm^3 versus FG S1, 22.0 ± 6.5 mm^3; $P < 0.001$).

Effect of PDGF-BB overexpression on tumor cell proliferation and apoptosis. To determine the effect of PDGF-BB overexpression on tumor cell proliferation, tumors were stained for BrdU incorporation. There was a significant reduction in the number of proliferating tumor cells in the PDGF-BB–overexpressing tumors compared with the control tumors (HT-29 S2 tumors had approximately 56% as many proliferating cells per high-power field as did the control tumors; HT-29 S4 tumors had approximately 63% as many; $P < 0.01$) (Table 1). To determine the effect of PDGF-BB overexpression on apoptosis, tumor sections were stained for TUNEL. There were no statistically significant differences in the number of TUNEL-positive cells in tumors from the various groups, although there was a trend toward increased TUNEL staining in the PDGF-B–transfected cell lines (Table 1).

Effect of PDGF-BB overexpression on microvessel counts and pericyte-like cells. Immunohistochemical staining of the tumor vasculature revealed inhibition of microvessel counts proportional to the relative overexpression of PDGF-BB (Table 1). On average, microvessel counts in PDGF-BB–expressing tumors were only 41% of those in control tumors ($P < 0.02$). Tumor sections were also stained for EC proliferation (CD31/BrdU) and EC apoptosis (CD31/TUNEL). EC apoptosis was exceedingly rare in all of the tumor specimens (data not shown). There was a trend toward decreased EC proliferation in the PDGF-BB–overexpressing tumors; however, this trend did not reach statistical significance (Table 1).

Since the receptor for PDGF-BB (PDGFRβ) is highly expressed on pericytes, we investigated the effect of PDGF-BB overexpression on the relative numbers of pericytes within tumors. Recent reports suggest that pericytes express a number of different markers and that no single marker is definitive in identifying pericytes; therefore, we stained for numerous pericyte markers, including PDGFRβ, NG2, desmin, and α-SMA (12, 14). The data suggested that there was a significant increase in the number of pericytes and pericyte precursor cells within the PDGF-BB–overexpressing tumors (Figure 2 and Supplemental Video 1; available online with this article; doi:10.1172/JCI31334DS1). We quantified the amount of pericyte coverage using 2 markers (desmin and NG2) in combination with CD31 to stain for ECs and demonstrated that there is increased pericyte coverage in the PDGF-BB–overexpressing tumors (Table 1).

PDGFRβ has also been shown to be expressed in cells within the stromal compartment of tumors. To determine whether the PDGF-BB–overexpressing cells led to an increase in stromal tumor content, Gomori trichrome staining was performed on tumors derived from the HT-29 parental, Neo pool, S2, and S4 cell lines. There was no significant difference in the amount of stromal tissue content within tumor as determined by a gastrointestinal pathologist in a blinded fashion (data not shown).

Effect of PDGF-BB overexpression on tumor growth in the liver. Since tumor growth and angiogenesis are influenced by the organ micro-

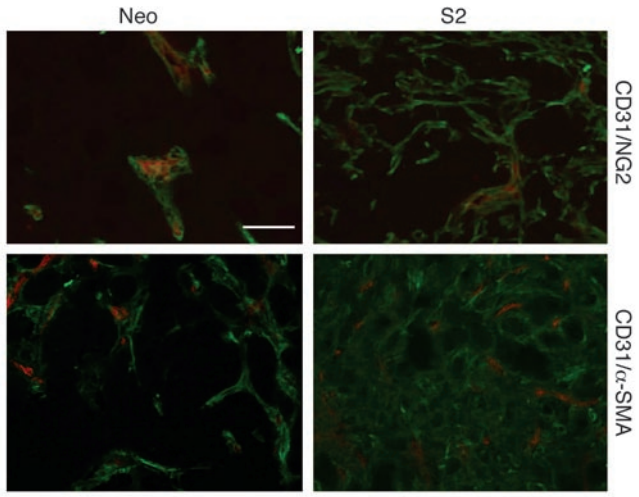

Figure 2
Effect of PDGF-BB overexpression on pericyte coverage. HT-29 tumor sections from mice injected with HT-29 control (Neo pool) or PDGF-BB–overexpressing (S2) cells were double stained for ECs (CD31; red) and pericyte markers (NG2 and α-SMA; green). There was an increased influx of pericytes or pericyte-like cells within the PDGF-BB–overexpressing tumors. Representative photomicrographs are shown for the HT-29 Neo pool and the HT-29 S2 groups. Scale bar: 50 μm.

Table 2
Effect of PDGF-BB overexpression on tumor growth and weight in the orthotopic environment

Liver	HT–29 Neo pool	HT-29 S2	HT-29 S4
Tumor incidence, no. of mice	9/10 (90%)	4/10 (40%)	3/10 (30%)[A]
Tumor volume, mm^3 (mean ± SEM)	423 ± 120	45 ± 29[B]	13 ± 11[C]
Tumor mass, g (mean ± SEM)	0.25 ± 0.06	0.06 ± 0.03[C]	0.02 ± 0.01[C]
Pancreas	**FG Neo pool**	**FG–S1**	
Tumor incidence, no. of mice	14/14 (100%)	1/14 (7%)[C]	
Tumor volume, mm^3 (mean ± SEM)	3,349 ± 1,400	0.0 ± 0.0[C]	
Tumor weight, g (mean ± SEM)	2.0 ± 0.8	0.0 ± 0.0[C]	

[A]$P < 0.03$ by χ^2 test versus Neo pool. [B]$P < 0.02$ by Student's *t* test versus Neo pool. [C]$P < 0.007$ by Student's *t* test versus Neo pool.

environment, and since the liver is the preferred site of metastasis of CRC, HT-29 parental, vector-transfected, and PDGF-B–transfected tumor cells were injected into the livers of nude mice (22). On day 36, mice in the control group began to show signs of lethargy, and thus all mice were sacrificed. Tumor incidence was decreased by 50%–60% in the mice injected with PDGF-BB–overexpressing cells (Table 2). In addition, the average tumor weight among the tumor-bearing mice was decreased by 58%–79% in the mice injected with PDGF-B–transfected clones compared with the control mice ($P < 0.05$) (Table 2 and Figure 3). Tumor volume was also significantly decreased (~86% to 91%) in the mice injected with PDGF-B–transfected clones ($P < 0.05$) (Table 2).

Effect of PDGF-BB overexpression on tumor growth in the pancreas. We then sought to determine the impact of PDGF-BB overexpression on the growth of FG pancreatic tumors in the orthotopic environment. Therefore, FG Neo pool and FG S1 (PDGF-BB–overexpressing tumor cells) were injected into the pancreata of nude mice. On day 103, all mice were sacrificed because of tumor burden in the control group. Tumor incidence was decreased by 93% in the mice injected with PDGF-BB–overexpressing cells (Table 2) ($P < 0.001$). In addition, the average tumor weight in the tumor-bearing mice was 99% lower in the mice injected with PDGF-BB–overexpressing clones than in the control mice ($P < 0.001$). Tumor volume was also significantly decreased in the mice injected with PDGF-BB–overexpressing clones (Table 2) ($P < 0.001$).

Effect of PDGF-BB overexpression on pericyte-like cell function. To determine the in vitro effect of PDGF-BB–overexpressing tumor cells on pericytes, a variety of cell proliferation, migration, and coculture assays were performed utilizing VSMCs, as these are believed to be the in vivo precursors to pericytes. As shown in Figure 4A, conditioned medium from the PDGF-BB–overexpressing clones significantly increased proliferation of human VSMCs by almost 2-fold ($P < 0.01$). Conditioned medium from the control or vector-transfected cells did not increase VSMC proliferation. These results were confirmed in an experiment using 10T 1/2 murine mural/pericyte-like cells (data not shown). In a cell migration assay in which HT-29 cells were placed in the lower chamber of a modified Boyden chamber, migration of VSMCs from the upper to the lower chamber was significantly greater in the presence of the PDGF-overexpressing clones (Figure 4B; $P < 0.05$).

Effect of pericyte-like cells on EC proliferation in coculture. Since our in vivo studies demonstrated a decrease in tumor growth and an increase in pericyte content in mice injected with PDGF-BB–overexpressing tumor cells, we sought to determine whether pericyte-like cells regulate EC proliferation, as has been suggested by previous work from the laboratory of D'Amore and colleagues (8, 23, 24). Pericyte-like cells and HUVECs were prestained using fluorescent markers. Following staining with fluorescent markers, cells were cultured in vitro with (a) unstained cells of the same type or (b) unstained 10T 1/2 cells as a coculture. The total number of cells per well remained the same. After 48 hours, the cells were sorted and quantified by FACS. The number of HUVECs in cocultures with pericyte-like cells was decreased by 47% compared with the number of HUVECs cultured with HUVECs only (Figure 5). This effect was only observed when cells were grown so as to allow cell-cell contact; this effect was not observed when cells were cultured in Boyden chambers (data not shown). These data suggested that pericyte-like cells are capable of inhibiting EC proliferation and that this inhibition of EC proliferation by pericytes requires cell-cell contact. In similar studies done with cocultures of 10T 1/2 and CRC cells, we did not observe any growth inhibition of CRC cells by pericyte-like cells (data not shown).

Effect of inhibition of PDGFR activity on tumor growth and pericyte content in vivo and tumor cell number in vitro. To determine whether tumor growth inhibition due to PDGF-BB overexpression was mediated by activation of PDGFR, imatinib mesylate was utilized to block PDGFR activity in vivo. Control vector transfectants (HT-29 Neo pool) and PDGF-BB–overexpressing cells (HT-29 S2) were injected subcutaneously into nude mice, and mice were treated with either imatinib mesylate or solvent (water; control). Similar to what was observed in the above studies, overexpression of PDGF-BB led to a marked inhibition of tumor growth (Figure 6).

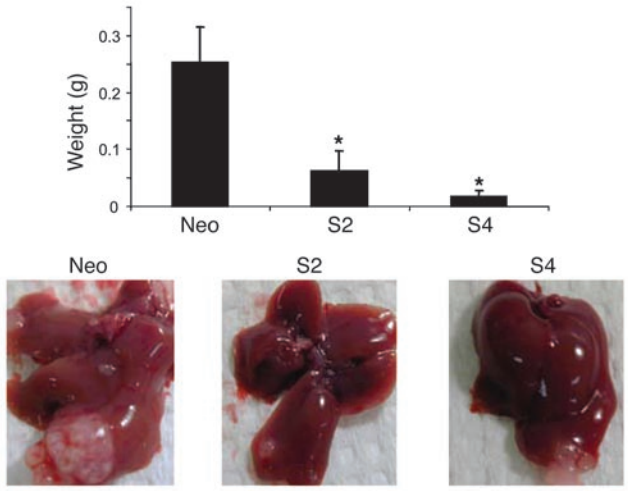

Figure 3
Effect of PDGF-BB overexpression on tumor growth in the liver. HT-29 control (Neo pool), and PDGF-BB–overexpressing (S2 and S4) cells (1×10^6) were injected directly into the livers of nude mice. Mice were sacrificed, and the tumors were measured and weighed. There was a significant reduction in tumor mass in the PDGF-BB–overexpressing tumors. *$P < 0.001$. Original magnification, ×1.

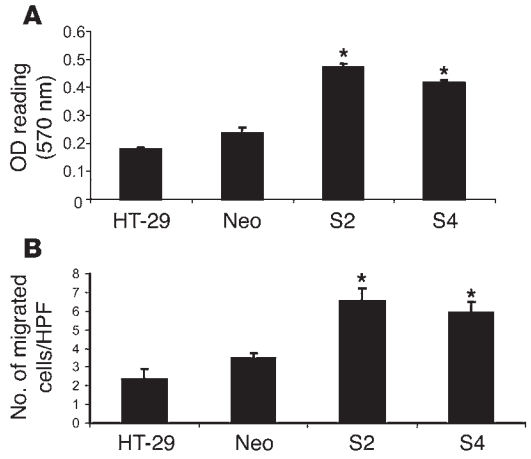

Figure 4
Effect of PDGF-BB overexpression in HT-29 cells on VSMCs. (**A**) Conditioned medium from HT-29 parental, control (Neo pool), and PDGF-BB–overexpressing (S2 and S4) cell lines was plated onto VSMCs for 72 hours. MTT analysis was then performed. There was increased proliferation of VSMCs in response to conditioned medium from PDGF-BB–overexpressing HT-29 cells relative to controls. (**B**) Tumor cells were then plated in the bottom of a modified Boyden chamber and allowed to adhere overnight. VSMCs were plated on top and were allowed to migrate for 24 hours in response to the tumor cells. We observed an increase in VSMC migration in response to the PDGF-BB–overexpressing HT-29 cells relative to controls. HPF, high-power field. *$P < 0.05$.

Daily therapy with imatinib mesylate partially reversed the growth inhibition observed with PDGF-BB overexpression. Compared with the mice injected with PDGF-BB–overexpressing cells and treated with solvent, mice injected with PDGF-BB–overexpressing cells and treated with imatinib mesylate exhibited a 56% increase in tumor growth (Figure 6). There was no statistically significant difference between the growth of the Neo pool tumors in mice treated with imatinib mesylate and the growth of the Neo pool tumors in mice treated with solvent alone (Figure 6). The experiment was repeated, and similar results were obtained.

HT-29 Neo pool and HT-29 S2 tumors were stained for pericyte markers, and pericytes were visualized using confocal microscopy. There was an increased influx of pericytes in PDGF-BB–overexpressing tumors compared with control tumors (Figure 2), and this influx was markedly decreased in mice treated with imatinib mesylate (Figure 7). Analysis of pericyte coverage also demonstrated decreased attachment of pericytes to ECs in the presence of imatinib mesylate therapy (Table 1).

In vitro studies were performed to determine whether PDGF-BB–overexpressing tumor cells were as susceptible to imatinib mesylate as were control cells. There were no differences in cell number or IC_{50} among HT-29 parental, HT-29 Neo pool, HT-29 S2, and HT-29 S4 cells treated in a dose-dependant fashion with various concentrations of imatinib mesylate (data not shown). These data suggest that the effects observed in vivo were not due to a direct effect of PDGF-BB on tumor cells themselves.

Discussion

In this study, we demonstrated that overexpression of PDGF-BB by human CRC and pancreatic cancer cells inhibited tumor growth in vivo. Neither the HT-29 human CRC cells nor the FG human pancreatic cancer cells expressed detectable levels of PDGF-BB or showed altered proliferation with the addition of PDGF-BB. Transfection of the *PDGFB* gene into HT-29 or FG cells resulted in selective overexpression of PDGF-BB but not of the heterodimer PDGF-AB. There was a significant increase in the number of pericytes in the PDGF-BB–overexpressing tumors concomitant with a decrease in the microvessel counts of these tumors compared with control tumors. In vitro studies demonstrated that pericyte-like cells are able to inhibit EC proliferation. Treatment with imatinib mesylate, a tyrosine kinase inhibitor of PDGF-Rβ, resulted in a partial reversal of the tumor growth inhibition in mice injected with HT-29 PDGF-BB–overexpressing transfectants. The imatinib mesylate–treated tumors also demonstrated a decreased number of pericytes, again suggesting that pericytes mediate tumor growth inhibition, possibly through their inhibition of EC proliferation.

The PDGF/PDGFR system has previously been shown to be directly involved in oncogenic transformation (25, 26). PDGF-B was the first growth factor shown to be a viral oncogene (PDGF-B/*v-sis*) (25). Many of the studies demonstrating the oncogenic role of PDGF-B were initially done in murine cell lines (such as NIH3T3) (25, 26). In human cell lines, the oncogenic properties of PDGF-B are more difficult to demonstrate (27). There is extensive evidence for the overexpression of PDGF-B/PDGFRβ in tumors of neuroectodermal origin leading to enhanced tumor growth and progression (28). There is also evidence implicating the growth-promoting effects of PDGF in other tumor types, including leukemia (29, 30), melanoma (31), mesothelioma (32), osteosarcoma (33, 34), breast cancer (35), and lung cancer (36).

Despite the wealth of literature on PDGF and PDGFR in other tumor types, there are comparatively few published data about the effects of PDGF-B/PDGFRβ in colorectal or pancreatic cancers. Elucidating the role of PDGF in these tumor types is important, since in our studies, there was no effect of PDGF-BB on either colon or pancreatic cancer cell proliferation in vitro. An initial study of PDGF/PDGFR in human colon cancer cell lines revealed that 67% expressed PDGF-B, but none expressed PDGFR at the mRNA level (37). Another study determined that only 33% of human colon adenocarcinoma cell lines expressed detectable levels of PDGF protein (38). Yet another study analyzing full-thickness

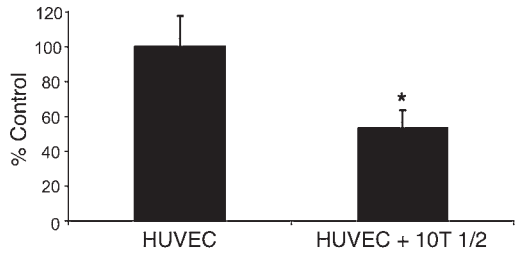

Figure 5
Inhibition of EC proliferation in vitro in the presence of pericytes. HUVECs and 10T 1/2 cells were labeled with fluorescent red or green dye. HUVECs were then plated onto a 6-well plate with either undyed HUVECs or 10T 1/2 cells. After 48 hours of coculture, cells were trypsinized, and HUVECs were sorted using FACS analysis. The total number of fluorescent red cells (HUVECs) was determined as a percentage of the control. 10T 1/2 cells inhibited HUVEC growth by almost 50% compared with cells that were in culture with unstained HUVECs. *$P < 0.05$.

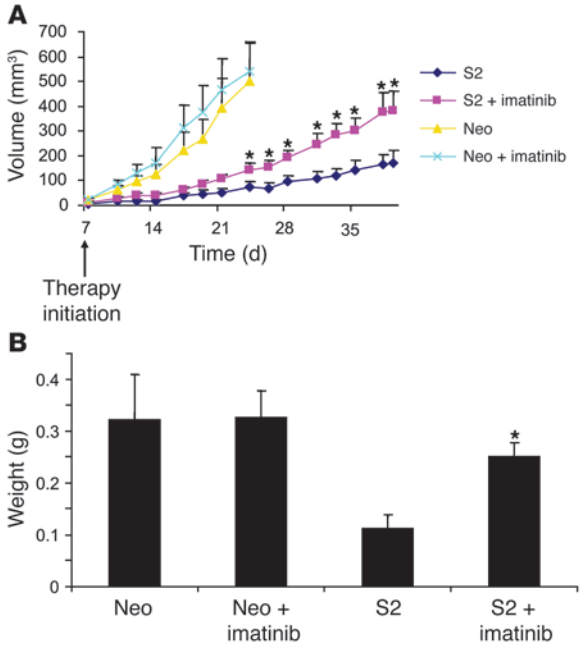

Figure 6

Effect of imatinib mesylate on tumor growth in vivo. HT-29 Neo pool and HT-29 S2 cells (1×10^6) were injected subcutaneously into nude mice. Imatinib mesylate was administered daily by oral gavage beginning on day 7. Treatment of PDGF-BB–overexpressing cells with imatinib mesylate increased tumor growth. (**A**) Volume. (**B**) Mass. *$P < 0.05$.

biopsy specimens from more than 200 human CRCs determined that PDGFRβ is expressed by stromal cells but not tumor epithelium (39). Finally, a recent article by Kitadai et al. demonstrated that PDGF-BB is expressed at moderate to high levels in human CRC specimens; however, PDGFRβ expression was only seen in 25% of the same cases (21). This provides additional evidence that the potential importance of the PDGF/PDGFR loop in the colon cancer microenvironment, unlike in neuroectodermal tumors, is paracrine, not autocrine, in nature. Human pancreatic cancer specimens demonstrate a pattern of PDGF and PDGFR expression similar to what is seen in CRC. One study of 13 human pancreatic tumors showed that, although PDGF-A was expressed by nearly all of the specimens, only 6 of 13 (46%) expressed low levels of PDGF-B as detected by mRNA (40). Another study of 5 human pancreatic adenocarcinomas showed expression of PDGF-A, PDGF-B, PDGFRα, and PDGFRβ in the cytoplasm of both ductal-like cancer cells and poorly differentiated cancer cells by immunohistochemical analysis (41). Given the small number of specimens tested in both of these studies, however, it is difficult to discern what role, if any, PDGF ligands may play in the growth and metastasis of pancreatic cancer.

The current study demonstrated that induced overexpression of PDGF-BB in tumors led to an increase in pericytes within tumors and a decrease in tumor growth. Our in vitro corollary studies suggested that the observed reduction in tumor growth might be due to pericyte-mediated inhibition of EC proliferation. Importantly, although previous studies have also reported an increase in pericytes associated with PDGF-BB overexpression, our study is the first to our knowledge to associate PDGF-BB overexpression with an increase in pericytes that results in *decreased* tumor growth. In a study by Guo et al., transfection of PDGF-BB into glioblastoma cells led to increased pericyte coverage and *enhanced* angiogenesis and tumor growth in the brain microenvironment (42). The discrepancies between our findings and those of Guo et al. are most likely due to the presence of PDGFR on glioblastoma cells and differences in the tumor microenvironment. The U87MG glioblastoma cells used in the study by Guo et al. express high levels of PDGFRβ, which is phosphorylated in response to PDGF-BB (42). In contrast, in our study, HT-29 colon cancer cells did not demonstrate activation of the receptor in response to ligand activation. Therefore, it is probable that in the glioblastoma cells, the activation of an autocrine loop resulted in increased tumor cell proliferation, and this enhanced proliferation might overcome growth inhibition mediated by the recruitment of pericytes. In a study by Abramsson et al., overexpression of PDGF-BB in fibrosarcoma cells also led to increased pericyte coverage in vivo (43). In their study, though, the PDGF-BB–overexpressing cells exhibited a slight decrease in in vivo tumor growth compared with the control cells, although this difference was not statistically significant (43). The authors attributed this decrease to clonal variation. Ongoing studies in our laboratory have suggested that the amount of PDGF-BB produced by different tumor cell lines may determine the growth rate in vivo: in these studies, tumors that express the highest amount of PDGF-BB in vitro have the slowest tumor growth rate in vivo (data not shown).

Data from the current study demonstrate that pericyte-like cells grown in vitro are able to inhibit EC proliferation. Thus, this study confirms previous work suggesting that one function of pericytes is to inhibit the growth of ECs (8, 24). The mechanism of action for this inhibition has been reported to be mediated both by direct cell-cell contact and through the production of soluble mediators such as TGF-β1 (8, 44).

In the current study, treatment of HT-29 tumors with imatinib mesylate, a known inhibitor of PDGF-βR (as well as c-Kit and Abl), resulted in different effects on tumor growth in control and PDGF-BB–overexpressing tumors. As in previously published studies in which this compound was tested against epithelial tumors (45), imatinib mesylate had no effect on the growth of HT-29 control tumors. Other studies have demonstrated that imatinib mesylate has little or no effect on tumor growth in vivo even though this agent demonstrates significant antiproliferative effects in vitro (45). Strikingly, however, in our studies, treatment of the PDGF-BB–overexpressing tumors with imatinib mesylate partially reversed the PDGF-BB–mediated growth-inhibitory effects. We hypothesize that the mechanism by which this occurred was reversal of pericyte-mediated inhibition of EC proliferation. Pericytes and VSMCs express high levels of the PDGFRβ and are targets for this tyrosine kinase inhibitor. Imatinib mesylate treatment of all tumor cell lines (HT-29 parental, HT-29 Neo pool, HT-29 S2, HT-29 S4) in vitro was able to significantly decrease growth (data not shown). Thus, the fact that imatinib mesylate partially reversed the growth-inhibitory effects of PDGF-BB in vivo is most likely due to an alteration in cells in the host tumor microenvironment. These data indicate the importance of understanding cell-specific expression of PDGF-B and PDGFRβ in tumors treated with inhibitors of this pathway.

In human tumors, pericytes are localized to the periendothelial cell location, since vessel maturation depends on not only PDGFR ligands but other EC-derived angiogenic mediators such as angiopoietin-1. Although aberrations in pericyte recruitment in tumors

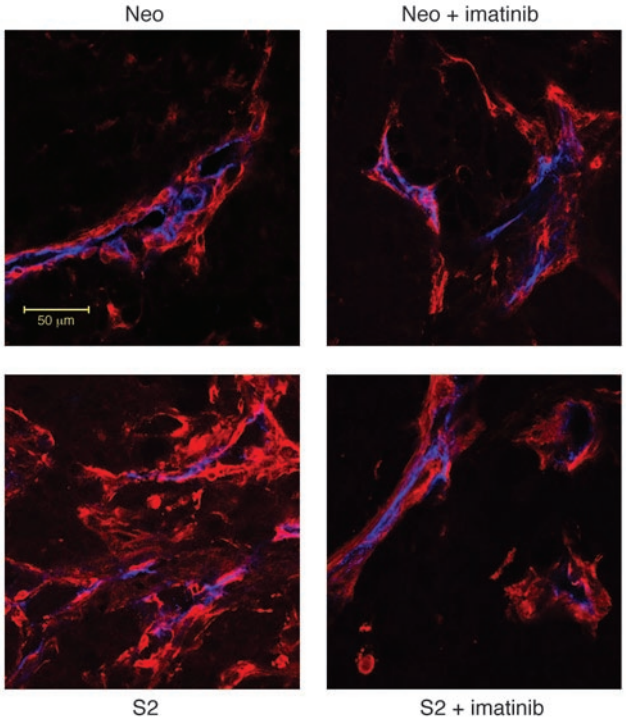

Figure 7
Effect of imatinib mesylate on pericyte coverage of HT-29 tumors. HT-29 tumors were double-stained for ECs and pericyte markers. NG2 staining (red) was used as a marker of pericytes or pericyte-like cells, whereas CD31 (blue) was used to identify ECs. There was an increased influx of NG2-positive cells within the PDGF-BB–overexpressing tumors, similar to what was shown previously (Figure 2). This influx was reduced in the imatinib mesylate–treated group, in which pericyte coverage appeared similar to that in control tumors. Representative photomicrographs are shown for each group. Scale bar: 50 μm.

overexpressing PDGF-BB may occur, this has not been analyzed in detail in human tumors due to the difficulty in studying numerous pericyte markers simultaneously. However, we recognize that forced expression of PDGF-BB to the level observed in our studies may not reflect the level observed in the majority of tumor types in patients.

In conclusion, our data demonstrate that overexpression of PDGF-BB in human CRC and pancreatic cancer cells results in decreased tumor growth. PDGF-BB–overexpressing tumors are characterized by an increase in the relative proportions of pericyte (and possibly pericyte precursor) cells. In vitro studies confirmed that pericytes have the ability to decrease EC proliferation, suggesting that one function of pericytes is to regulate EC growth. Additional studies utilizing imatinib mesylate in vivo demonstrated decreased pericyte coverage and adherence in the treated tumors and thus confirmed the role of PDGF-BB in increasing pericyte coverage within tumors. Also, imatinib mesylate partially reversed the growth inhibition in PDGF-BB transfectants, supporting the hypothesis that pericytes tightly control EC proliferation and angiogenesis within tumors.

Methods

Cell culture and transfection

Human cancer cell lines were either obtained from ATCC (HT-29, GEO, and RKO) or were the generous gifts of I.J. Fidler (The University of Texas MD Anderson Cancer Center) (KM12L4, KM12SM, and FG). All cell lines were cultured and maintained in modified Eagle medium supplemented with 10% FBS as described previously (22). HUVECs, VSMCs, and 10T 1/2 cells (murine mural/pericyte-like cells) were obtained from ATCC and cultured according to ATCC guidelines.

The full-length cDNA for PDGF-B was subcloned from the pSM-1 plasmid, obtained from ATCC, by digesting a 2.0-kb *Bam*HI fragment of the original plasmid and subcloning it into pcDNA3.1 (Invitrogen) containing a neomycin resistance gene. Vector alone or vector containing the *PDGFB* gene was transfected into HT-29 cells using FuGENE 6 (Roche Diagnostics) per the manufacturer's protocol, and the cells were grown in selective medium (10% modified Eagle medium plus 400 μg/ml neomycin; G418; Life Technologies Inc.).

For in vivo studies, HT-29 and FG cells transfected with PDGF-B and mock-transfected with pcDNA were harvested from subconfluent cultures. Briefly, cells were rinsed with PBS solution, trypsinized (0.25% trypsin, 0.1% EDTA), and resuspended in modified Eagle medium containing 10% FBS. Cells were counted, and cell viability was assessed using the trypan blue exclusion assay (>90% viability). Cells were resuspended in HBSS for tumor inoculation into nude mice.

ELISA for PDGF-AA, PDGF-AB, and PDGF-BB

HT-29 and FG cells were plated at 10^6 cells per 6-well plate and allowed to attach overnight. Fresh medium (1% modified Eagle medium) was added to the cultures, and cells were cultured for 72 hours. Medium was harvested, spun at 210 *g*, filtered using a 0.22-μm filter, and frozen at –20°C until needed. Cells were counted using the trypan blue exclusion assay, and ELISAs were performed per the manufacturer's instructions (R&D Systems).

Cell proliferation and cell-cycle analysis of transfected cells

MTT assay. A stock solution was prepared by dissolving 5 mg of MTT (3-[4,5-dimethylthiazol-2-yl]-2,5-diphenyl tetrazolium bromide; M2128; Sigma-Aldrich) in 1 ml of PBS and filtering the solution to remove particulates. The solution was protected from light, stored at 4°C, and used within 1 month. Cells were seeded into 96-well plates in triplicate and allowed to adhere overnight. The cultures were then washed, and medium was changed, exposing cells to PDGF-BB (10 ng/ml) or control. After 24, 48, and 72 hours, absorbance was determined by MTT assay. After 2 hours of incubation in medium containing 0.42 mg/ml of MTT, the cells were lysed in dimethyl sulfoxide. The conversion of MTT to formazan by metabolically viable cells was monitored by an MR-5000 96-well microtiter plate reader at 570 nm (Dynatech Inc.).

FACS analysis. FACS analysis was performed to detect potential changes in cell cycle in transfected cell lines. Cells were grown to approximately 50% confluence, washed in PBS, and fixed in 70% ethanol overnight at 4°C. Propidium iodide supplemented with RNase was added, and 30 minutes later, FACS analysis was performed using an EPICS XL-MCL flow cytometer (Beckman Coulter) with a 488-nm argon ion laser. Green fluorescence was detected at 520 nm, and red fluorescence was detected at 575 nm.

To determine whether EC proliferation is inhibited by the presence of pericyte-like cells, HUVECs and 10T 1/2 cells were dyed fluorescent red (HUVEC) or fluorescent green (10T 1/2) according to the manufacturer's protocol (PKH67/PKH26 Fluorescent Cell Linker Kit; Sigma-Aldrich). HUVECs (red; 50,000 cells) were then plated with an equal number of undyed cells or 10T 1/2 cells (green; 50,000 cells). After 48 hours of coculture, HUVECs were trypsinized and sorted using FACS analysis, and the total number of fluorescent red cells was determined.

Cell migration assay

The effects of tumor cell–secreted PDGF-BB on VSMC migration in vitro were investigated using a modified Boyden chamber (BD Biosciences) with uncoated inserts (8.0-μm pores). VSMCs or 10T 1/2 cells were plated into migration inserts (50,000 cells per insert in 1% medium), and HT-29 parental, HT-29 Neo pool, HT-29 S2, or HT-29 S4 cells (50,000 cells in 1% medium) were plated into the bottom wells. Inserts were plated in triplicate for each cell line and incubated for 24 hours at 37°C. Migrating cells were stained (DiffQuick; Dade Behring), and 5 random fields were counted per insert at ×50 magnification.

Animal studies

Eight-week-old male athymic nude mice (obtained from the National Cancer Institute Animal Production Area) were acclimated for 1 week and caged in groups of 5. All animal studies were approved by the Animal Care and Use Committee of the MD Anderson Cancer Center.

Subcutaneous studies. HT-29 or FG cells (10^6) in HBSS were injected into the subcutaneous space on the flanks of nude mice. Tumor growth was monitored and measured with calipers 3 times per week. Approximately 1 hour prior to sacrifice, mice were injected intraperitoneally with 1 mg of BrdU. When mice became moribund, they were sacrificed by CO_2 asphyxiation. Mice were weighed, and tumors were excised and weighed. Tumor tissue was harvested and either placed in 10% buffered formalin for paraffin fixation or frozen in OCT compound (Miles Inc.) in liquid nitrogen for subsequent immunohistochemical analysis.

Direct liver injection. The preferential metastatic site for CRC is the liver. Therefore, we have developed a technique for directly injecting tumor cells into the liver (22). Mice were anesthetized using methoxyflurane (Medical Developments International) and, under sterile conditions, subjected to an upper midline laparotomy. HT-29 cells (10^6) were injected under the capsule into the lateral lobe of the liver. Tumors were allowed to grow until mice became moribund. Mice were sacrificed via CO_2 asphyxiation and weighed, and the liver was excised. Total liver weight (including liver tumors) was determined, and tumors were carefully dissected free of surrounding liver, measured, and weighed. Tumor tissue was harvested and processed as described above.

Intrapancreatic injection. For intrapancreatic injections, mice were anesthetized using methoxyflurane (Medical Developments International) and, under sterile conditions, subjected to a left flank incision, as previously described (46). FG cells (10^6) were injected into the tail of the pancreas. Tumors were allowed to grow until mice became moribund. Mice were sacrificed via CO_2 asphyxiation and weighed, and the pancreas was excised. Total pancreatic weight (including pancreatic tumors) was determined, and tumors were carefully dissected free of surrounding pancreas, measured, and weighed. Tumor tissue was harvested and processed as described above.

Anti-PDGFR therapy. Imatinib mesylate (Gleevec/STI-571) was manufactured by Novartis. Mice were injected subcutaneously with HT-29 cells (5×10^5). Four days later, mice were administered imatinib mesylate 50 mg/kg daily or water (control) by oral gavage. Tumor growth was monitored daily and measured 3 times per week using calipers. Mice were sacrificed, and organs were harvested as described above.

Immunostaining of microvessels, pericytes, and tumor cell proliferative and apoptotic markers

Tissues were sectioned and stained for H&E, CD31 (vessels), α-SMA (pericytes), desmin (pericytes), NG2 (pericytes), TUNEL (apoptotic cells), and BrdU (proliferative cells) as previously described (22). All tumor tissues were either counterstained with Gill's 3 hematoxylin (Sigma-Aldrich; immunohistochemical analysis) or incubated with 300 μg/ml of Hoechst stain for 1 to 2 minutes (Sigma-Aldrich; immunofluorescence analysis). Dual immunofluorescence staining was achieved by serially incubating the specimens in the desired antibodies. The antibodies used were as follows: rat anti-mouse CD31 (BD Biosciences — Pharmingen), mouse anti-human α-SMA (Dako), rabbit anti-desmin (Dako), rabbit anti-NG2 (Chemicon), mouse anti-BrdU (BD), rat anti-PDGFRβ (eBioscience), DeadEnd Fluorometric TUNEL system (Promega), rat anti-mouse IgG_{2a} (Serotec), Texas red goat anti-rat secondary antibody (Jackson ImmunoResearch Laboratories Inc.), and goat anti-mouse IgG Alexa Fluor 488 (Molecular Probes; Invitrogen).

Analyses of immunostained tissue sections

Immunostained tissue sections were examined using a Zeiss photomicroscope equipped with a 3-chip charge-coupled device color camera (DXC-960 MD; Sony Corp.). The images were analyzed using Optimas image analysis software (version 5.2). Positive cells were counted using Scion software based on the NIH image program for Macintosh (Scion Corp.). The number of positive cells was expressed as the average of the number of cells in 0.05-mm^2 high-power fields at ×200. Five fields per tumor section from either 8-μm-thick sections (BrdU, TUNEL) or 20-μm-thick sections (CD31, desmin, α-SMA, NG2) were chosen randomly, and 5 or more specimens per group were analyzed. Areas of obvious necrosis (as determined by either H&E or Hoechst counterstain) were excluded from analysis. To determine the percentage of vessel area, sections were analyzed using Optimas software. The cross-sectional area of CD31-positive structures (i.e., vessel area) was also determined in the same 4 quadrants by capturing images, converting them to grayscale, and analyzing the NG2/CD31-stained areas with NIH ImageJ software (version 1.62; http://rsb.info.nih.gov/ij/) by setting a consistent threshold for all slides so that only CD31-stained cells were apparent. The NG2/CD31-positive area was then expressed as the number of pixels squared per high-power field.

Statistics

Statistical differences among groups were examined using the 2-tailed Student's *t* test, the χ^2 test, or, for analysis of nonparametric data, the Mann-Whitney *U* test with InStat Statistical Software (GraphPad Software). The results of the in vivo experiments were tested for outliers using Grubb's test (www.graphpad.com). A *P* value of less than 0.05 was considered statistically significant.

Acknowledgments

The authors wish to acknowledge Stanley Hamilton, Department of Pathology, MD Anderson Cancer Center, for his assistance in reviewing the histology of the specimens; and Rita Hernandez, Department of Surgical Oncology, and Stephanie Deming, Department of Scientific Publishing, for editorial assistance.

Received for publication December 26, 2006, and accepted in revised form May 8, 2007.

Address correspondence to: Lee M. Ellis, Department of Surgical Oncology, Unit 444, The University of Texas MD Anderson Cancer Center, PO Box 301402, Houston, Texas 77230-1402, USA. Phone: (713) 792-6926; Fax: (713) 792-4689; E-mail: lellis@mdanderson.org.

1. Ellis, L.M. 2003. A targeted approach for antiangiogenic therapy of metastatic human colon cancer. *Am. Surg.* **69**:3–10.
2. Jung, Y.D., et al. 2002. The role of the microenvironment and intercellular cross-talk in tumor angiogenesis. *Semin. Cancer Biol.* **12**:105–112.
3. von Tell, D., Armulik, A., and Betsholtz, C. 2006. Pericytes and vascular stability. *Exp. Cell Res.* **312**:623–629.
4. Gerhardt, H., and Betsholtz, C. 2003. Endothelial-pericyte interactions in angiogenesis. *Cell Tissue Res.* **314**:15–23.

5. Sims, D.E. 2000. Diversity within pericytes. *Clin. Exp. Pharmacol. Physiol.* **27**:842–846.
6. Reinmuth, N., et al. 2001. Induction of VEGF in perivascular cells defines a potential paracrine mechanism for endothelial cell survival. *FASEB J.* **15**:1239–1241.
7. Antonelli-Orlidge, A., Saunders, K.B., Smith, S.R., and D'Amore, P.A. 1989. An activated form of transforming growth factor beta is produced by cocultures of endothelial cells and pericytes. *Proc. Natl. Acad. Sci. U. S. A.* **86**:4544–4548.
8. Orlidge, A., and D'Amore, P.A. 1987. Inhibition of capillary endothelial cell growth by pericytes and smooth muscle cells. *J. Cell Biol.* **105**:1455–1462.
9. Hammes, H.P., et al. 2002. Pericytes and the pathogenesis of diabetic retinopathy. *Diabetes.* **51**:3107–3112.
10. Benjamin, L.E., Golijanin, D., Itin, A., Pode, D., and Keshet, E. 1999. Selective ablation of immature blood vessels in established human tumors follows vascular endothelial growth factor withdrawal. *J. Clin. Invest.* **103**:159–165.
11. Eberhard, A., et al. 2000. Heterogeneity of angiogenesis and blood vessel maturation in human tumors: implications for antiangiogenic tumor therapies. *Cancer Res.* **60**:1388–1393.
12. Morikawa, S., et al. 2002. Abnormalities in pericytes on blood vessels and endothelial sprouts in tumors. *Am. J. Pathol.* **160**:985–1000.
13. Darland, D.C., et al. 2003. Pericyte production of cell-associated VEGF is differentiation-dependent and is associated with endothelial survival. *Dev. Biol.* **264**:275–288.
14. Bergers, G., Song, S., Meyer-Morse, N., Bergsland, E., and Hanahan, D. 2003. Benefits of targeting both pericytes and endothelial cells in the tumor vasculature with kinase inhibitors. *J. Clin. Invest.* **111**:1287–1295. doi:10.1172/JCI200317929.
15. Gee, M.S., et al. 2003. Tumor vessel development and maturation impose limits on the effectiveness of anti-vascular therapy. *Am. J. Pathol.* **162**:183–193.
16. Shaheen, R.M., et al. 2001. Tyrosine kinase inhibition of multiple angiogenic growth factor receptors improves survival in mice bearing colon cancer liver metastases by inhibition of endothelial cell survival mechanisms. *Cancer Res.* **61**:1464–1468.
17. Allt, G., and Lawrenson, J.G. 2001. Pericytes: cell biology and pathology. *Cells Tissues Organs.* **169**:1–11.
18. Betsholtz, C., Karlsson, L., and Lindahl, P. 2001. Developmental roles of platelet-derived growth factors. *Bioessays.* **23**:494–507.
19. Lindahl, P., Johansson, B.R., Leveen, P., and Betsholtz, C. 1997. Pericyte loss and microaneurysm formation in PDGF-B-deficient mice. *Science.* **277**:242–245.
20. Soriano, P. 1994. Abnormal kidney development and hematological disorders in PDGF beta-receptor mutant mice. *Genes Dev.* **8**:1888–1896.
21. Kitadai, Y., et al. 2006. Expression of activated platelet-derived growth factor receptor in stromal cells of human colon carcinomas is associated with metastatic potential. *Int. J. Cancer.* **119**:2567–2574.
22. Stoeltzing, O., et al. 2003. Angiopoietin-1 inhibits vascular permeability, angiogenesis, and growth of hepatic colon cancer tumors. *Cancer Res.* **63**:3370–3377.
23. D'Amore, P.A., and Sweet, E. 1987. Effects of hyperoxia on microvascular cells in vitro. *In Vitro Cell Dev. Biol.* **23**:123–128.
24. Hirschi, K.K., Rohovsky, S.A., Beck, L.H., Smith, S.R., and D'Amore, P.A. 1999. Endothelial cells modulate the proliferation of mural cell precursors via platelet-derived growth factor-BB and heterotypic cell contact. *Circ. Res.* **84**:298–305.
25. Josephs, S.F., et al. 1984. Transforming potential of human c-sis nucleotide sequences encoding platelet-derived growth factor. *Science.* **225**:636–639.
26. Clarke, M.F., et al. 1984. Transformation of NIH 3T3 cells by a human c-sis cDNA clone. *Nature.* **308**:464–467.
27. Potapova, O., Fakhrai, H., Baird, S., and Mercola, D. 1996. Platelet-derived growth factor-B/v-sis confers a tumorigenic and metastatic phenotype to human T98G glioblastoma cells. *Cancer Res.* **56**:280–286.
28. Westermark, B., Heldin, C.H., and Nister, M. 1995. Platelet-derived growth factor in human glioma. *Glia.* **15**:257–263.
29. Golub, T.R., Barker, G.F., Lovett, M., and Gilliland, D.G. 1994. Fusion of PDGF receptor beta to a novel ets-like gene, tel, in chronic myelomonocytic leukemia with t(5;12) chromosomal translocation. *Cell.* **77**:307–316.
30. Tsai, L.H., et al. 1994. Expression of platelet-derived growth factor and its receptors by two pre-B acute lymphocytic leukemia cell lines. *Blood.* **83**:51–55.
31. Westermark, B., et al. 1986. Human melanoma cell lines of primary and metastatic origin express the genes encoding the chains of platelet-derived growth factor (PDGF) and produce a PDGF-like growth factor. *Proc. Natl. Acad. Sci. U. S. A.* **83**:7197–7200.
32. Klominek, J., Baskin, B., and Hauzenberger, D. 1998. Platelet-derived growth factor (PDGF) BB acts as a chemoattractant for human malignant mesothelioma cells via PDGF receptor beta-integrin alpha3beta1 interaction. *Clin. Exp. Metastasis.* **16**:529–539.
33. Graves, D.T., et al. 1984. Detection of c-sis transcripts and synthesis of PDGF-like proteins by human osteosarcoma cells. *Science.* **226**:972–974.
34. Betsholtz, C., Westermark, B., Ek, B., and Heldin, C.H. 1984. Coexpression of a PDGF-like growth factor and PDGF receptors in a human osteosarcoma cell line: implications for autocrine receptor activation. *Cell.* **39**:447–457.
35. Yi, B., Williams, P.J., Niewolna, M., Wang, Y., and Yoneda, T. 2002. Tumor-derived platelet-derived growth factor-BB plays a critical role in osteosclerotic bone metastasis in an animal model of human breast cancer. *Cancer Res.* **62**:917–923.
36. Kawai, T., Hiroi, S., and Torikata, C. 1997. Expression in lung carcinomas of platelet-derived growth factor and its receptors. *Lab. Invest.* **77**:431–436.
37. Ito, M., et al. 1990. Expression of several growth factors and their receptor genes in human colon carcinomas. *Virchows Arch. B Cell Pathol. Incl. Mol. Pathol.* **59**:173–178.
38. Anzano, M.A., Rieman, D., Prichett, W., Bowen-Pope, D.F., and Greig, R. 1989. Growth factor production by human colon carcinoma cell lines. *Cancer Res.* **49**:2898–2904.
39. Lindmark, G., et al. 1993. Stromal expression of platelet-derived growth factor beta-receptor and platelet-derived growth factor B-chain in colorectal cancer. *Lab. Invest.* **69**:682–689.
40. Ebert, M., et al. 1995. Induction of platelet-derived growth factor A and B chains and over-expression of their receptors in human pancreatic cancer. *Int. J. Cancer.* **62**:529–535.
41. Hwang, R.F., et al. 2003. Inhibition of platelet-derived growth factor receptor phosphorylation by STI571 (Gleevec) reduces growth and metastasis of human pancreatic carcinoma in an orthotopic nude mouse model. *Clin. Cancer Res.* **9**:6534–6544.
42. Guo, P., et al. 2003. Platelet-derived growth factor-B enhances glioma angiogenesis by stimulating vascular endothelial growth factor expression in tumor endothelia and by promoting pericyte recruitment. *Am. J. Pathol.* **162**:1083–1093.
43. Abramsson, A., Lindblom, P., and Betsholtz, C. 2003. Endothelial and nonendothelial sources of PDGF-B regulate pericyte recruitment and influence vascular pattern formation in tumors. *J. Clin. Invest.* **112**:1142–1151. doi:10.1172/JCI200318549.
44. Darland, D.C., and D'Amore, P.A. 2001. TGF beta is required for the formation of capillary-like structures in three-dimensional cocultures of 10T1/2 and endothelial cells. *Angiogenesis.* **4**:11–20.
45. McGary, E.C., et al. 2002. Inhibition of platelet-derived growth factor-mediated proliferation of osteosarcoma cells by the novel tyrosine kinase inhibitor STI571. *Clin. Cancer Res.* **8**:3584–3591.
46. Camp, E.R., et al. 2006. Roles of nitric oxide synthase inhibition and vascular endothelial growth factor receptor-2 inhibition on vascular morphology and function in an in vivo model of pancreatic cancer. *Clin. Cancer Res.* **12**:2628–2633.